



INSTRUMENT CALIBRATION REPORT

HaloSat-001-CALDB-01

Version 1.0

DATE April 14, 2020

Goddard Space Flight Center
Greenbelt, Maryland

Prepared by: Anna Zajczyk (HaloSat/GSFC), Philip Kaaret and Rebecca Ringuette
(HaloSat/University of Iowa), Lorella Angelini (HEASARC/NASA)

Table of Contents

1	Introduction.....	4
1.1	Purpose.....	4
1.2	Science Instrument.....	4
1.3	Energy calibration.....	4
1.4	Response and effective area calculations.....	7
2	Release CALDB 20200129.....	9
2.1	Data Analysis	9
3	References.....	10

CHANGE RECORD PAGE

DOCUMENT TITLE : HaloSat-001-CALDB-01			
ISSUE	DATE	PAGES AFFECTED	DESCRIPTION
Version 1.0	April 2020	All	First release

1 Introduction

1.1 Purpose

This document describes how the *PI* were assigned in the ground software and how the response matrices in the caldb files were derived. The structure of the CALDB files are defined in the document halosat_caldb_v20200312 and available from the CALDB web page at https://heasarc.gsfc.nasa.gov/docs/heasarc/caldb/halosat/docs/halosat_caldb_docs.html.

1.2 Science Instrument

The HaloSat science instrument is made of three identical detector units. An Amptek, Inc. silicon drift detector (SDD) equipped with a C-series C1 window is used as an X-ray sensing element in each of the detector units. During nominal operation the silicon X-ray sensing element of each SDD is actively cooled to -30°C to achieve good energy resolution (<100 eV at 600 eV). The temperatures of the sensing element and the frontend electronics are measured every 8 seconds and written into the instrument housekeeping data. Detector units are referred to using numbers encoded in their digital processing units which are 14, 54 and 38.

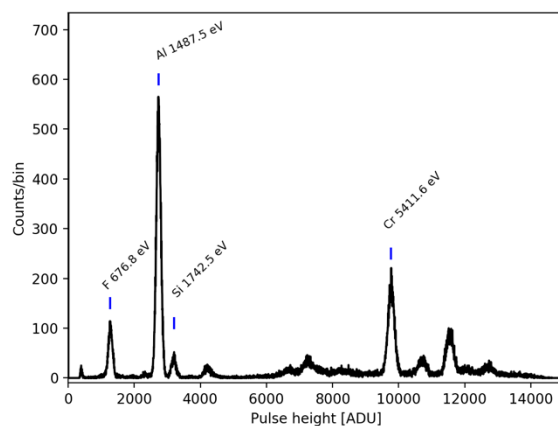


Figure 1. Calibration spectrum acquired during TVAC tests. The emission lines used to determine the energy calibration are labeled.

1.3 Energy calibration

The HaloSat science instrument underwent a series of thermal-vacuum (TVAC) tests in order to determine an energy calibration solution for its detector units. During each of the TVAC tests, the instrument temperature was varied between -25°C and 45°C and X-ray spectra were recorded with individual detector units. An X-ray tube illuminating a Teflon target was used in the tests. Figure 1

shows an example of a calibration spectrum obtained during the TVAC tests. Four strong and isolated emission lines were used to determine the energy calibration. The chosen lines are indicated in the figure marked with the element producing the line and its energy in eV.

Table 1. Temperature-dependent energy calibration coefficients for HaloSat detector units SDD 14, 38 and 54. For all detector units temperature dependence of C1 coefficient can be approximated with parabola $C1 = a1 \cdot T^2 + a2 \cdot T + a3$, while dependence of C2 can be approximated with linear function $C2 = a1 \cdot T + a2$. Derived values (and fit error) for a-coefficients are given in table below. Temperature T is the temperature given by the baseplate temperature sensor reported in the housekeeping data file (BPL_TEMP) for each of the detector units separately.

SDD 14			
		value	error
C1	a1	0.0000018615	0.0000002713
	a2	0.0000058429	0.0000106005
	a3	0.5437512278	0.0001179509
C2	a1	-0.1426338885	0.0097877002
	a2	-29.9819221014	0.2860704456

SDD 38			
		value	error
C1	a1	0.0000023380	0.0000001343
	a2	-0.0000472094	0.0000027445
	a3	0.5564678190	0.0000689721
C2	a1	-0.1355792938	0.0096806085
	a2	-32.9267861288	0.2121595317

SDD 54			
		value	error
C1	a1	0.0000006617	0.0000002371
	a2	-0.0000147105	0.0000107862
	a3	0.5493653560	0.0001358776
C2	a1	-0.1809170943	0.0120826882
	a2	-35.5069756003	0.3989365948

It was assumed that the pulse height to energy conversion can be approximated with a linear function $E = C1 \cdot PHA + C2$, where PHA is the pulse height of a recorded event, E is the photon energy corresponding to that event, and $C1$ and $C2$ are the slope and intercept of the linear function. For each TVAC spectrum obtained at each temperature used during the calibration, the centroids of the four emission peaks were measured and values of $(C1, C2)$ were obtained via least-squares linear fit. To parameterize the temperature dependence of the energy calibration, we examined the behavior of the $C1$ and $C2$ coefficients as a function of temperature¹. We found that the temperature dependence of the $C1$ coefficients can be well approximated with parabola and that of the $C2$ coefficients with a linear function. Table 1 shows parameters of the temperature-dependent energy calibration for the HaloSat detector units.

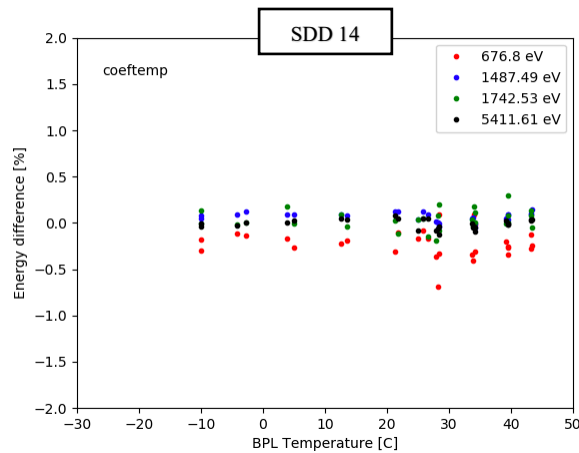


Figure 2. Relative difference (given in %) between the expected peak position and the peak position measured in the energy-calibrated spectrum as a function of instrument temperature. Shown here is behavior for SDD 14. All units show similar behavior.

Figure 2 shows a plot of the relative difference between the expected peak position and the peak position measured in a spectrum calculated using the temperature-dependent energy calibration given in Table 1. Results for four emission lines (F, Al, Si, and Cr) are shown. The average value of the peak position difference for fluorine line (676.8 eV) is 0.22% (1.49 eV), 0.28% (1.90 eV) and 0.16% (1.08 eV) for SDD 14, 38 and 54, respectively. Similarly, for chromium line (5411.61 eV) the values are 0.009% (0.49 eV), 0.009% (0.49 eV) and 0.014% (0.76 eV) for SDD 14, 38 and 54, respectively. These values represent accuracy of the energy calibration solution derived for the HaloSat science instrument.

The PHA (pulse height) to PI (pulse invariant) transformation is performed on all event files prior to their delivery to HEASARC. The following steps are necessary to convert PHA to PI :

¹ Each detector unit has a temperature sensor mounted on a detector's baseplate. The temperature measured by this baseplate sensor (referred to as a baseplate temperature BPL_TEMP in the housekeeping data) is used as a proxy for the temperature of the detector unit. For each detector unit the baseplate temperature is used to study the temperature dependence of $(C1, C2)$ coefficients.

1. Transformation from *PHA* to *E* – First, the temperature of the detector unit at the event arrival time is found.² Then, using the information given in Table 1 the values of (*C1*, *C2*) coefficients are calculated and the energy of the event (in eV) is obtained with the formula

$$E = C1 \cdot PHA + C2$$

2. Transformation from *E* to *PI* – the energy of the event is converted to the pulse invariant *PI* value following:

$$PI = \text{floor}(1 + (E/1000 - 0.1)/0.02)$$

In this formula:

- the energy of the event *E* is given in eV, and *E*/1000 converts it to keV;
- 0.1 keV is the adjustment for the minimum energy in the binning of the response;
- 0.02 keV is the bin size in the response;
- use of the *floor* function truncates decimal part.

This process is performed for each detector unit separately.

1.4 Response and effective area calculations

Because of very small differences in performance of the three detector units a single response file and a single effective area file are used to model detectors' behavior. All HaloSat response files are written in a format compatible with the XSpec spectral fitting software.

The response of the HaloSat SDDs is calculated with a version of the Scholze & Prokop (2009) code modified to model the response of the SDDs used by NASA's Neutron star Interior Composition Explorer (NICER) instrument. This version of the code was kindly provided to us by Dr. Jack Steiner of MIT. The SDDs used by HaloSat are identical to those used by NICER except for the type of the entrance window and the dimensions of the internal collimator. HaloSat calibration data where detector units were illuminated with ⁵⁵Fe radioactive source and the information on C1 window provided to us by Amptek, Inc. and HS Foils, Oy were used to adjust relevant detector parameters in the response simulation code (e.g. composition of the detector entrance window and electronic noise level).

Figure 3 shows an ⁵⁵Fe calibration spectrum and simulated response for one of the HaloSat detectors. This example shows that the data is well reproduced by the model: two photo peaks at 5.9 keV and 6.5 keV, silicon escape peaks at around 4.1 keV and 4.8 keV, Al and Si instrumental lines originating from detector entrance window, and line tails/shelves that extend towards low energies and arising from charge loss effects in the detector. Given the limitations of our calibration data, the shape of the noise peak present below 400 eV was not modelled, and thus, this sets low energy limit to the accuracy of the calculated response for HaloSat. The upper limit of about 7 keV is set by the properties of our signal processing electronics.

² The events are binned into 8-second bins, with the bin edges created to match the time bins in the housekeeping data. The time corresponding to the lower edge of the bin is used to find the corresponding baseplate temperature (a proxy for the detector unit temperature), and this temperature is then assigned to all events in the bin.

The effective area of each HaloSat detector unit was determined from calculations that account for transmission through C-series C1 window, transmission through Amptek’s Multilayer Collimator (MLC), transmission through the SDD’s dead layer, and absorption in the SDD’s active volume. The information on the structure of Si sensor and the MLC provided by Amptek, Inc.³, and on the

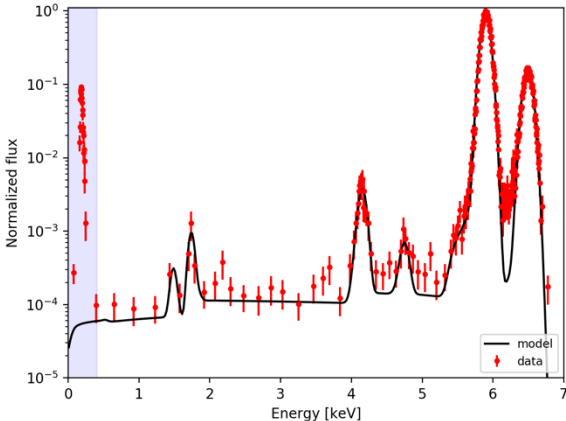


Figure 3. HaloSat ⁵⁵Fe calibration spectrum and simulated response. Shaded area shows region below 400 eV that is not covered by our response model.

C1 window properties provided by HS Foils, Oy⁴, were used in the calculations. The calculated effective area of a single HaloSat detector at the oxygen lines of primary interest for HaloSat is 4.301 mm² at 561 eV and 5.979 mm² at 653 eV. A plot of the effective area versus energy is shown in Figure 4.

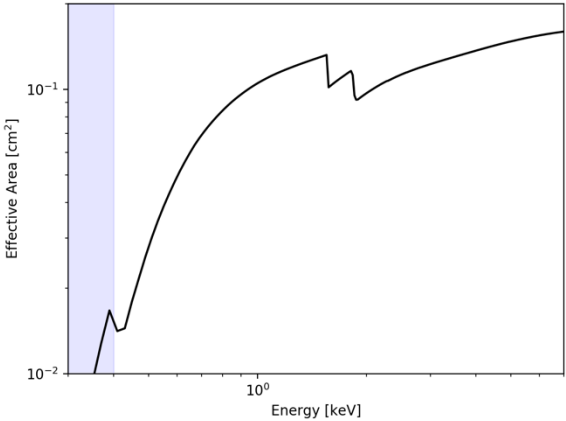


Figure 4. Effective area calculated for a single HaloSat detector unit. Shaded area shows region below 400 eV that is not covered by our response model.

³ Detailed information on Amptek’s silicon drift detectors can be found at <https://www.amptek.com/products/sdd-x-ray-detectors-for-xrf-eds/fast-sdd-silicon-drift-detector>.

⁴ Private communication with HS Foils, Oy, which is part of Amptek, Inc.

2 Release CALDB 20200129

Filename	Valid data	Release data	CALDB Vrs	Comments
<i>hs_sdd_align20180701v001.fits</i>	2018-07-01	20200320	20200129	
<i>hs_sdd_all20180701v001.arf</i>	2018-07-01	20200320	20200129	
<i>hs_sdd_avgnoise20180701v001.rmf</i>	2018-07-01	20200320	20200129	
<i>hs_sdd_diag20180701v001.rmf</i>	2018-07-01	20200320	20200129	

hs_sdd_align20180701v001.fits

File containing HaloSat pointing information.

hs_sdd_all20180701v001.arf

File containing effective area information. There is one ARF file and it is applicable to all HaloSat detector units.

hs_sdd_avgnoise20180701v001.rmf

Single response matrix file (RMF) is generated for HaloSat and it is applicable to all three detector units. Transformation from *PHA* to *PI* is not included in the RMF file. It is a separate step performed by HaloSat team with Python-based tools on raw data prior to their delivery to HEASARC. This approach simplifies the RMF generation process.

hs_sdd_diag20180701v001.rmf

Diagonal response matrix used to model HaloSat instrumental background. At the time of writing a power law model with the diagonal response matrix is used to model the instrumental background.

2.1 Data Analysis

TVAC data were analyzed using analysis tools developed by the HaloSat team. HaloSat analysis tools were written in Python.

Response files (ARF and RMF) were created using tools written in Python (HaloSat team) and in IDL (Scholze & Prokop code).

Design and construction of HaloSat science instrument is described in detail in LaRocca et al. (2020). On-ground calibration of the science instrument can be found in Zajczyk et al. (in preparation), while on orbit calibration is presented in Kaaret et al. (2019).

3 References

Kaaret et al., “HaloSat: a cubesat to study hot galactic halo”, 2019, ApJ, 884, 162

LaRocca et al., “Design and construction of the x-ray instrumentation onboard the HaloSat CubeSat”, 2020, JATIS, 6, 014003

Scholze and Prokop, “Modelling the response function of energy dispersive X-ray spectrometers with silicon detectors”, 2009, X-Ray Spectrometry, 38, 4

Zajczyk et al., “On-ground calibration of the HaloSat science instrument”, in preparation, to be submitted to JATIS